ELSEVIER

Journal of Structural Geology 28 (2006) 868–886

JOURNAL OF STRUCTURAL GEOLOGY

www.elsevier.com/locate/jsg

Influence of crustal heterogeneity on normal fault dimensions and evolution: southern South Africa extensional system

Douglas A. Paton [a,b,*]

[a] School of GeoSciences, The University of Edinburgh, The King's Buildings, West Mains Road, Edinburgh EH9 3JW, UK
[b] Section 4.3, GeoForschungsZentrum Potsdam, Telegrafenberg, 14473 Potsdam, Germany

Received 10 December 2004; received in revised form 23 December 2005; accepted 21 January 2006
Available online 3 April 2006

Abstract

The tectonic configuration of southern South Africa is dominated by a continental scale, Mesozoic extensional system superimposed upon a significant, and well constrained, Palaeozoic lithospheric scale heterogeneity. Through integrating onshore structural analysis with offshore subsurface studies it is possible to evaluate the applicability of established normal fault growth models in a heterogeneous crustal setting at a basin scale for the first time. The >480-km-long Mesozoic extensional system comprises a number of fault arrays that vary in length from 78 to 230 km. Coupled with displacements of up to 16 km, the fault arrays are amongst the longest and largest displacement of high angle normal faults (dips of 45–60°) documented in continental lithosphere, although comprised of co-linear segments rather than the en-échelon segment configuration typical of many other extensional systems. This atypical geometry is considered to be a consequence of the high degree of structural inheritance between the underlying Paleozoic Cape Fold Belt and the subsequent extensional system. Furthermore, it is proposed that the overall displacement–length dimensions of the extensional faults were inherited from the underlying compressional faults. The establishment of a seismic–stratigraphic framework for the Pletmos and Gamtoos offshore basins reveals that the faults established their long lengths (160 and 90 km, respectively) within ~6 Myr of rift initiation prior to accruing their substantial displacement (16 km). Furthermore, there is no evidence for the development of intra-basin faults.

The southern South Africa extensional system presents an end member case of structural inheritance where extensional structures are parallel to and reactivate underlying compressional structures. In this study structural inheritance is considered to have a significant effect on mechanisms of fault growth. The pre-existing structures not only result in the rapid establishment of fault lengths of up to 160 km, but, additionally, to strain being localised onto the pre-existing fabric to such an extent that no intra-basin faults evolve and strain is accommodated entirely on the bounding faults.

Keywords: Normal faults; Reactivation; Fault growth; Crustal heterogeneity; South Africa

1. Introduction

Significant advances have been made over the last decade to the understanding of rift basins and the alterations that occur to their structural configuration during active extension (e.g. Cartwright et al., 1995; Dawers and Anders, 1995; Marchal et al., 1998; Cowie et al., 2000; Dawers and Underhill, 2000; McLeod et al., 2000; McClay et al., 2002). Two commonly cited end-member mechanisms that characterise fault growth are radial tip propagation of isolated fault segments and linkage between neighbouring segments (e.g. Walsh and Watterson, 1988; Cowie and Scholz, 1992a,b; Dawers et al., 1993; Anders and Schlische, 1994; Trudgill and Cartwright, 1994; Cartwright et al., 1995). However, many recent studies in numerical and analogue modelling (e.g. Gupta et al., 1998; Marchal et al., 1998; Cowie et al., 2000; McClay et al., 2002), field studies (e.g. Cartwright et al., 1995; Dawers and Anders, 1995; Sharp et al., 2000) and subsurface studies utilising high resolution 3D seismic datasets (e.g. Morley, 1999; Dawers and Underhill, 2000; Contreras et al., 2000; McLeod et al., 2000, 2002) suggest a spectrum between the two end-members. The majority of these models propose that rift initiation is typically dominated by a large population of small displacement, short, isolated fault segments. During subsequent extension, strain is progressively localised onto a few, long faults through the interaction of tip propagation and segment linkage. The rift climax is characterised by a small population of large displacement basin-bounding faults (Cowie et al., 2000).

* Correspondence address: Section 4.3, GeoForschungsZentrum Potsdam, Telegrafenberg, 14473 Potsdam, Germany.
E-mail address: paton@gfz-potsdam.de.

0191-8141/$ - see front matter © 2006 Published by Elsevier Ltd.
doi:10.1016/j.jsg.2006.01.006

Associated with these studies, fault systems have been characterised from a statistical viewpoint and the power law relationship:

$$D = cL^n$$

describing the relationship between displacement (D) and length (L), where c is a constant and n is a scaling exponent, is commonly invoked. The value of n has been much debated with values ranging from 0.5 (Fossen and Hesthammer, 1997) to 1 (Cowie and Scholz, 1992a,b; Dawers et al., 1993) to 1.5 (Walsh and Watterson, 1988; Gillespie et al., 1992; Dawers et al., 1993; Schlische et al., 1996), with a value of 1 commonly taken as a reasonable approximation. Although often applied, such a relationship defines a static fault population and does not predict how an individual fault, or fault array, will evolve through time. A number of studies have discussed that during the evolution of a single fault system such a relationship might not be applicable (Walsh et al., 2002; Bellahsen et al., 2003).

A further limitation of many of the currently proposed models is that the presence of pre-extensional faults, or structural fabric, within the continental lithosphere is not taken into account (e.g. McConnell, 1972; Ramberg, 1978; Illies, 1981; Morley, 1999; Lezzar et al., 2002; Bellahsen et al., 2003). A few recent studies have demonstrated that pre-existing faults and structural fabric can have a significant effect on fault development (e.g. Ebinger et al., 1999; Walsh et al., 2002; Paton and Underhill, 2004). Few settings, however, provide the juxtaposition of suitable high resolution data for an extensional basin evolution study with a well-constrained, and structurally reactivated, pre-extensional fault system. Southern South Africa provides such a setting, and this paper integrates high resolution onshore observations with offshore sub-surface data to investigate whether the pre-existing fabric influences (a) the length–displacement dimensions of extensional faults, and (b) the evolution of their spatial geometry through time.

1.1. Regional geology

The crystalline basement of southern South Africa is not exposed, with the oldest strata that crops out being the Neoproterozoic Pre-Cape metamorphosed sedimentary sequences, with locally intruded granitic bodies (Fig. 1). The sedimentary sequences were deposited into dominantly E–W-trending rift basins and are persevered as inliers within the Cape Fold Belt (Figs. 1 and 2; Shone et al., 1990; Tankard et al., 1982; Barnett et al., 1997).

Surrounding these inliers is the Cape Supergroup that comprises up to 8 km of siliciclastic continental margin sediments and is of Ordovician to Early Carboniferous in age (Figs. 1 and 2; Broquet, 1992; Booth and Shone, 1999). The Cape Supergroup is divided into three groups, which are, from youngest to oldest: the quartzites of the Table Mountain Group; the argillaceous fine grained sandstones of the Bokkeveld Group; and the shales and subordinate sandstones of the Witteberg Group (Figs. 1 and 2). The Table Mountain and Bokkeveld groups have the greatest areal occurrence and form the majority of the surface geology of the southern coastal area. In contrast, the Witteberg Group is limited to the northernmost extent of the Cape Supergroup exposure and is overlain unconformably to the north by the Late Paleozoic/Triassic Karoo Supergroup (Figs. 1 and 2; Tankard et al., 1982; Turner, 1999). The Karoo strata, which are only present to the north of the Cape Supergroup, comprise a 7000-m-thick succession of glacial, turbiditic and terrestrial deposits and consist of the Dwyka, Ecca and Beaufort groups (Figs. 1 and 2). The Karoo Supergroup corresponds to a foreland basin sequence that developed in response to lithospheric loading associated with

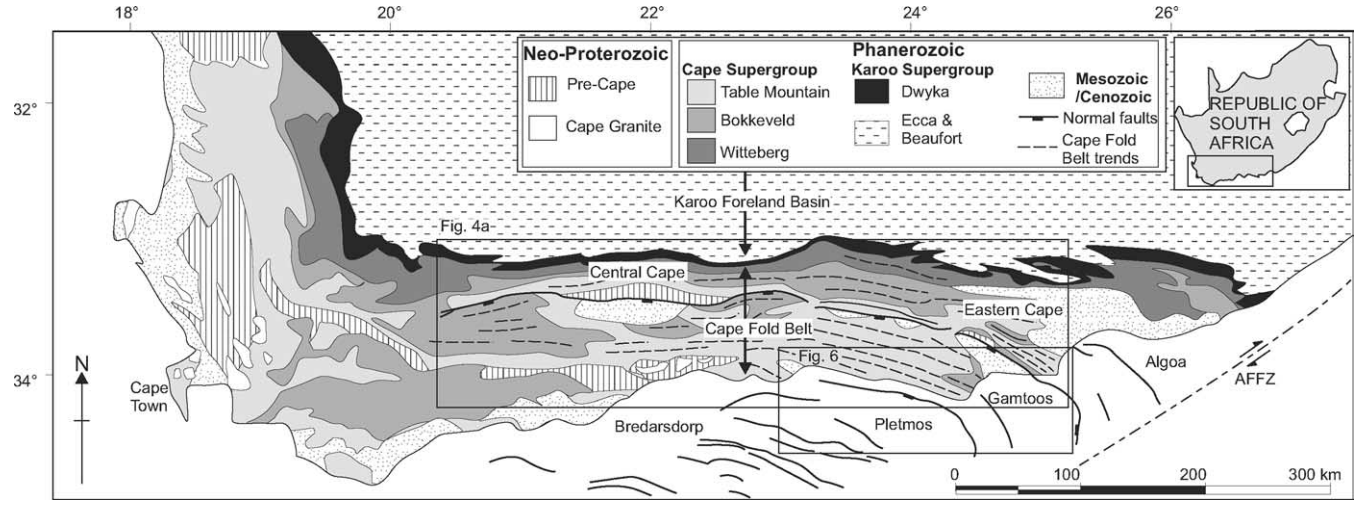

Fig. 1. Schematic geological map of southern South Africa. The principal units are: the Neo-Proterozoic, Pre-Cape strata that are preserved as inliers within the Cape Fold Belt; the clastic margin sequence of the Cape Supergroup that was deformed during the Permian–Triassic Cape Orogeny to form the Cape Fold Belt; the Karoo Supergroup that was deposited into the foreland basin associated with the Cape Orogeny; and the Mesozoic onshore sequence that was deposited into extensional faults during the subsequent negative structural inversion of the fold-belt. The correlation in trend of the Cape Fold Belt structural fabric and the Mesozoic extensional faults is evident in particular to the southeast where there is change in trend from an E–W orientation to a NW–SE trend of both the structural fabric and the extensional faults (after Dingle et al., 1983; Hälbich, 1993).

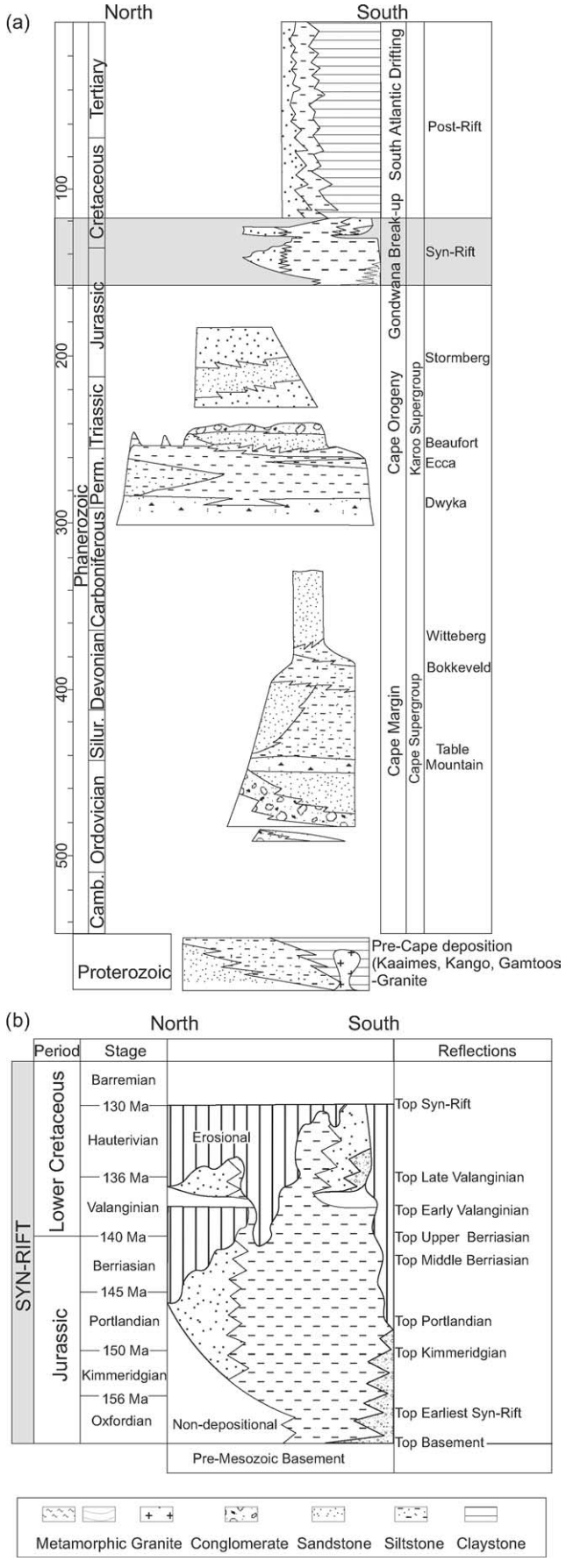

Fig. 2. Chronostratigraphy for southern South Africa including the principal pre-rift and syn-rift groups and supergroups. Inset highlights the syn-rift interval in more detail and includes the mapped seismic horizons (after Dingle et al., 1983; Veevers et al., 1994; McMillan et al., 1997; Catuneanu et al., 1998, 2005; Turner, 1999; Booth and Shone, 2002).

a Late Paleozoic Cape Orogeny (Cloetingh et al., 1992; Catuneanu et al., 1998, 2005). This orogeny generated the Cape Fold Belt, which deformed the Cape Supergroup in a series of E–W-trending and S-dipping thrusts, and dominates the structural configuration of southern South Africa (Fig. 1; Dingle et al., 1983; Hälbich, 1993).

During the break-up of Gondwana and the subsequent rifting of the South Atlantic, the negative structural inversion of the Cape Fold Belt resulted in the development of a series of Mesozoic age S-dipping normal faults. These faults bound a number of onshore outliers and four offshore basins (Bredarsdorp, Pletmos, Gamtoos and Algoa; Fig. 1; de Wit and Ransome, 1992, and references therein). This study investigates the onshore outliers and the Pletmos and Gamtoos basins. The oldest dated syn-rift sediments are Oxfordian and rifting is considered to have initiated in the Late Jurassic (Fig. 2; McMillan et al., 1997). The offshore basin fill is a terrestrially dominated earliest syn-rift interval overlain by an Oxfordian–Valanginian marine sequence that gradually coarsens-up from anoxic shales to continental shelf sandstones. The rift–drift transition is characterised by an Early Cretaceous basin-wide unconformity. Overlying the unconformity is the shallow marine post-rift sequence (Fig. 2; Bate and Malan, 1992; McMillan et al., 1997).

1.2. Nature of the Cape Fold Belt structural fabric

The geology of southern South Africa, and the Cape Fold Belt, records a series of tectonic episodes over the last 650 Myrs that utilise the same faults (Fig. 1; Dingle et al., 1983; de Wit and Ransome, 1992; Hälbich, 1993). Over the last decade a substantial number of studies have demonstrated the consistency across the fold belt of a N–NE verging compressional episode utilising E–W-trending and S-dipping reverse faults associated with the Late Paleozoic Cape Orogeny. Evidence for the deformation comes from: Pre-Cape foliations and metamorphic fabrics (Shone et al., 1990; Barnett et al., 1997); Cape Supergroup structures including fold axes, thrust planes, duplexes and imbrication orientations, cleavages and structural lineations (Coetzee, 1983; Hälbich et al., 1983; Hälbich, 1993; Booth and Shone, 1999, 2002); and Karoo Supergroup deformation (Catuneanu et al., 1998; Turner, 1999). These studies consistently highlight the E–W trend of the Cape Fold Belt structures in the central Cape with a change in orientation to NW–SE in the eastern Cape (Fig. 1).

It has also been extensively documented that there is a close correlation in trend of the Cape Fold Belt with the superimposed Mesozoic faults, and a number of workers have demonstrated the structural reactivation of some of the fold belt compressional faults during the Mesozoic extension

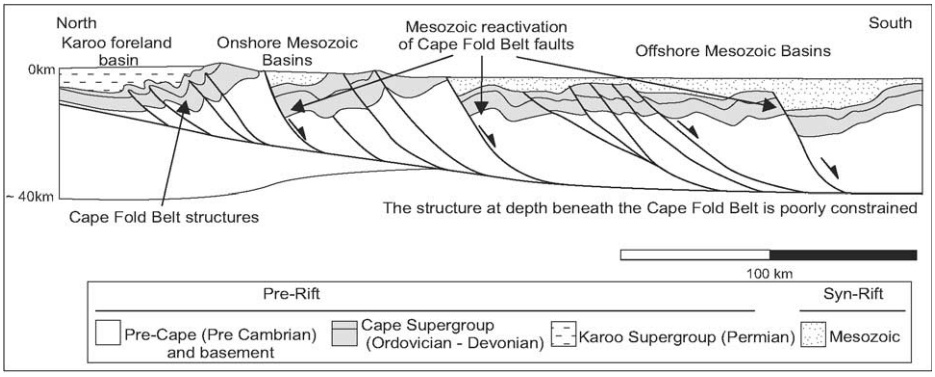

Fig. 3. Schematic cross-section through the Cape Fold Belt that demonstrates the well documented negative structural inversion of the Cape Fold Belt faults during the Mesozoic extension. This inversion has been demonstrated both onshore and offshore. Despite the well constrained nature of the inversion at a shallow crustal level, there remains uncertainty with respect to the accommodation of this inversion within the lower crust (after Hälbich, 1993).

(Fig. 3; Le Roux, 1983; Bate and Malan, 1992; Booth and Shone, 1992; de Wit and Ransome, 1992; Gresse et al., 1992; Newton, 1993; Booth, 1996). These extensional structures have a similar change in trend from NW-SE to N-S in the eastern Cape as documented for the Cape Fold Belt structures. What is more speculative is the depth within the lithosphere to which reactivation has occurred. Most studies are in agreement that the Cape Fold Belt structures were reactivated during the Mesozoic (de Wit and Ransome, 1992; Gresse et al., 1992; Hälbich, 1993; Booth and Shone, 2002) and a number have argued for a S-dipping mega-décollement that has undergone structural reactivation (e.g. Hälbich, 1993). The occurrence of a significant magnetic anomaly (Beattie Anomaly) and an electrically conductive zone (Southern Cape Conductive Belt) at the northern edge of the Cape Fold Belt was interpreted to be evidence of a lower crustal level mafic body and attributed to obducted oceanic crust on the mega-décollement (Hälbich, 1993). More recent studies have questioned the nature of the depth at which this body is located with some studies suggesting a shallower level for the body (e.g. Harvey et al., 2001). Given this uncertainty in the lower crustal configuration of the region, this study will focus solely on the influence of the reactivation of the Cape Fold Belt reverse faults during the Mesozoic extension.

1.3. Methods and data

The development of the southern South African extensional system was investigated using plan view fault geometry and depocentre evolution. Fault geometry was established through the identification of (a) along-strike variability of fault trend, (b) abrupt changes in fault trace, and (c) where possible, the geometry of the fault plane itself. The presence of the first two features is commonly attributed to the growth of faults whereby neighbouring fault segments with an en-échelon relationship link to form a throughgoing structure (e.g. Trudgill and Cartwright, 1994); this technique requires that the original segments are not co-linear. The resulting structure has a step in trace at the location of overlap between the original segments with an intra-basin high separating the hangingwall depocentres. A number of studies have demonstrated that through the identification of such features it is possible to reconstruct the progressive establishment of a fault system by determining a hierarchy of isolated segments (Dawers et al., 1993; Anders and Schlische, 1994; Trudgill and Cartwright, 1994; McLeod et al., 2000, 2002). As the location and extent of hangingwall depocentres are predominantly controlled by the bounding fault, sediment accumulation within the depocentre and the presence of displacement minima can be used to reconstruct subsidence and fault growth (e.g. McLeod et al., 2000).

In the onshore study area field observations and structural mapping were supplemented by mapping onto 30 m resolution ETM+ satellite images to investigate the relationship between the rift basins and the underlying Cape Fold Belt and the geometry of the normal faults associated with the sedimentary basins (Figs. 4a and 5).

The offshore sub-surface data comprise ~10,000 km of 2D seismic reflection sections with a vertical axis in milliseconds two-way travel time (ms TWT), maximum recording values of either 5000 or 6000 ms TWT, a 25 m shot point interval and a 60-fold geophone coverage (Figs. 6 and 7). Seismic reflection data were made available by the Petroleum Agency of South Africa (formerly SOEKOR). Seismic interpretation was based upon the determination of mega-sequences through the identification of seismic reflection geometries (e.g. downlap, onlap, erosional truncation; after Mitchum et al., 1977; Hubbard et al., 1985a,b). Mega-sequences were attributed to the broad classification of pre-rift, syn-rift or post-rift, defined by the nature of the internal geometries (after Prosser, 1993). The syn-rift interval was sub-divided into nine sequences with each sequence being conformable within a mega-sequence (Figs. 2 and 7). The onset of rifting occurred at approximately 162 Ma (McMillan et al., 1997) and ages of the syn-rift intervals were derived from biostratigraphic data from 27 exploration wells and are: Top Earliest Syn Rift >156 Ma; Top Kimmeridgian 150 Ma; Top Portlandian 145 Ma; Top Berriasian 140 Ma; Top Valanginian 136 Ma; Top Syn Rift 130 Ma (McMillan et al., 1997; Gradstein et al., 2004). The derived scheme is broadly similar to that of published

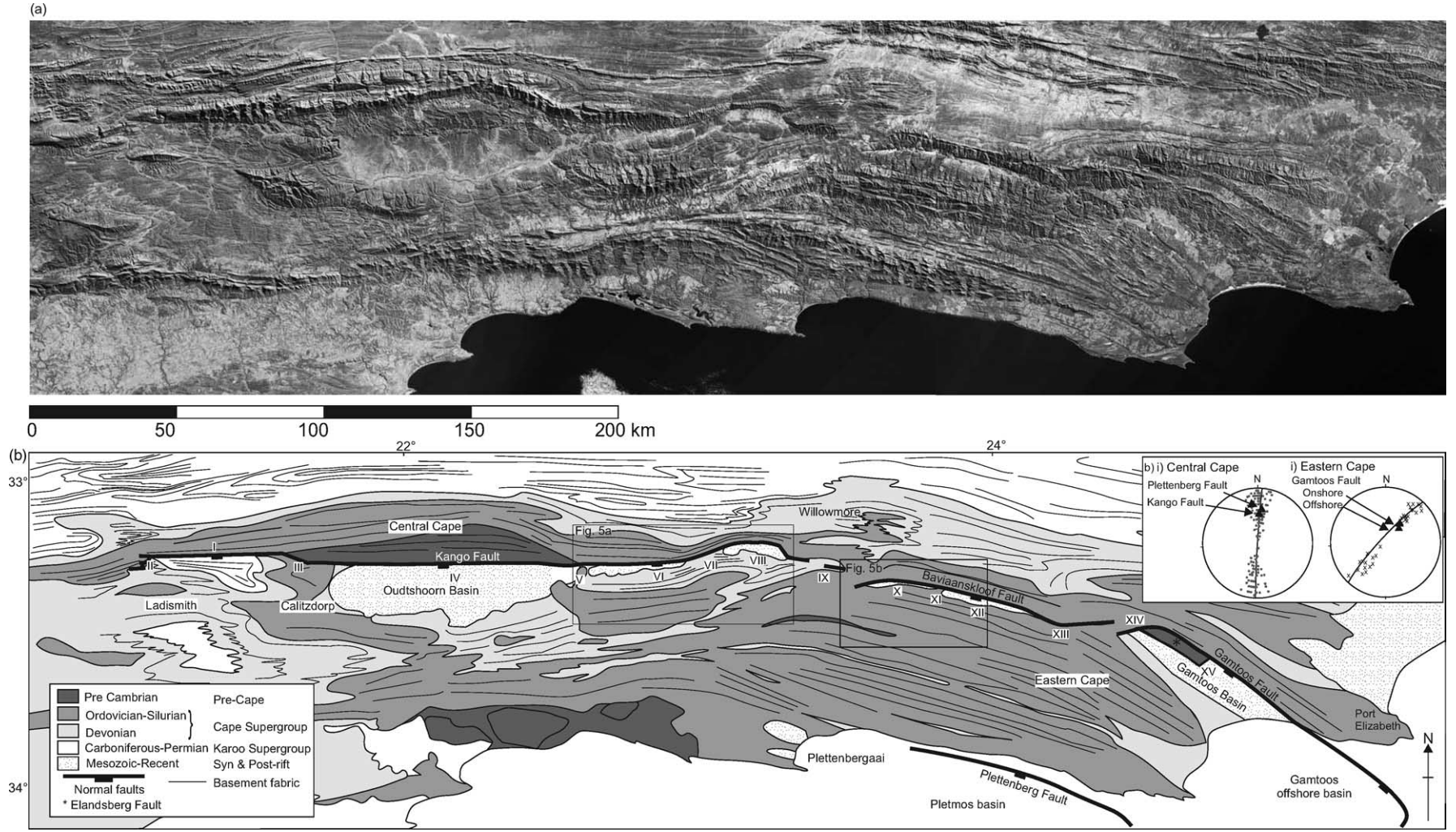

Fig. 4. (a) Compiled ETM+ Landsat images of southern South Africa with interpretation of the principal structural fabrics, stratigraphic units and location of the Mesozoic extensional faults (onshore and offshore) (after Dingle et al., 1983; McMillan et al., 1997; Paton, 2002; ETM+ images are WRS 2 and row/paths are: 173/084, 172/083, 172/084, 171/083, 171/084, 173/083. In addition, ETM+ Mosaics 071-690 and 071-697 were used). (b) Southern hemisphere stereonet with poles to planes of compressional structures (faults, folds and foliations) for (i) the Central Cape (circles), and (ii) the Eastern Cape (crosses). The poles to the Mesozoic faults have been plotted and demonstrate the well documented correlation in trend between pre-Mesozoic compressional and Mesozoic extensional structures.

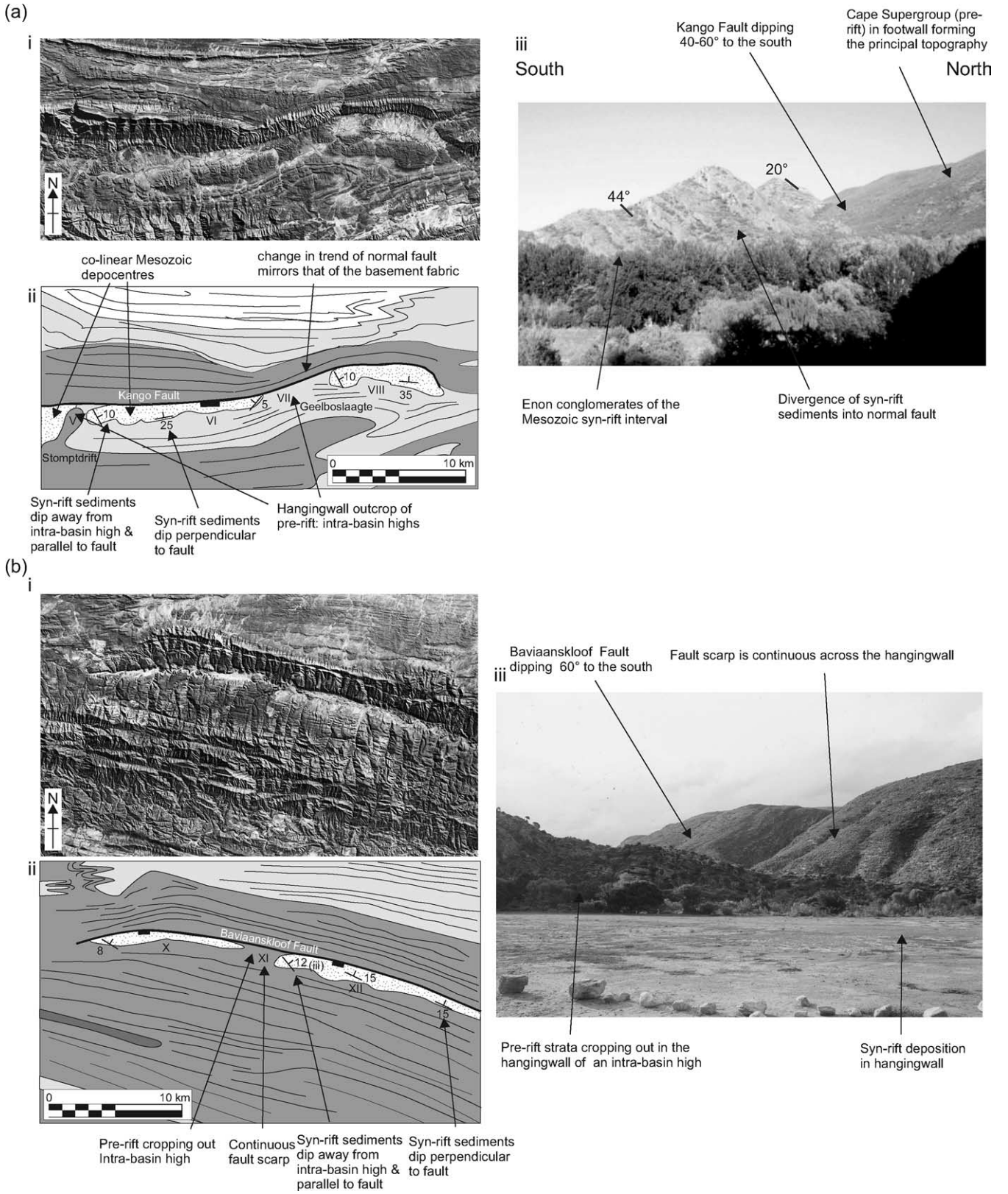

Fig. 5. (a) Kango Fault: (i) Enlargement of the eastern Kango Fault Landsat image, with (ii) interpretation, highlighting the presence of intra-basin highs separating Mesozoic depocentres and how the change in trend of the basement fabric is reflected in an identical change in trend in the Mesozoic fault (Fig. 4 for location). (iii) Photograph (viewed towards the west) shows thickening and divergence of syn-rift intervals into the Kango Fault. Sedimentologically, the syn-rift interval is comprised of interbedded red-bed conglomerates and sandstones. (b) Baviaanskloof Fault: (i) Enlargement of the western Baviaanskloof Fault Landsat image, with (ii) interpretation, demonstrating the co-linear nature of isolated depocentres in the immediate hangingwall to the fault (Fig. 4 for location). (iii) The view from the eastern depocentre towards the pre-rift exposure in the intra-basin high to the northwest. This view shows the continuous nature of the fault scarp (~200 m high) between Mesozoic depocentre and the intra-basin high.

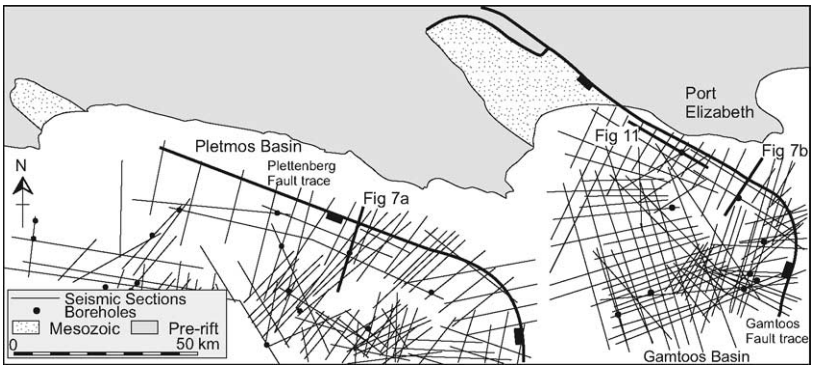

Fig. 6. Map of the offshore portion of the Mesozoic basins in the SE Cape showing the sub-surface data set utilised in the study of the Plettenberg and Gamtoos (offshore) faults; see Fig. 1 for location. The locations of the two faults are shown (derived from hangingwall cut-off locations).

SOEKOR data (Bate and Malan, 1992; McMillan et al., 1997). Interpreted horizons were subsequently gridded and contoured using Schlumberger IESX Geoframe 7.1 software to produce 3D surfaces. Isochron plots (thickness in TWT) were calculated to determine variations in sediment accumulation in space and time. The high quality of the seismic data, coupled with the large impedance contrast between the siltstone dominated syn-rift interval and quartzitic basement, resulted in well-imaged fault plane positions, facilitating the mapping of fault plane surfaces.

2. Fault system development

2.1. Geometry and displacement/length of the bounding faults

The study of the geometry of the bounding faults to the extensional basins was separated into: (1) plan view geometry and fault length analysis; and (2) cross-sectional geometry and displacement determination.

2.1.1. Plan view geometry and fault lengths

The onshore portion of the extensional system comprises three fault arrays: the Kango, Baviaanskloof and Gamtoos, from west to east, respectively (Fig. 4a). The fault arrays are defined by S-dipping normal faults with sedimentary basins in their hangingwalls. A number of previous studies have demonstrated that the Mesozoic faults are co-linear to the Cape Fold Belt structural fabric and commonly reactivate pre-existing fold-belt compressional faults (Le Roux, 1983; Bate and Malan, 1992; Booth and Shone, 1992, 1999; de Wit and Ransome, 1992; Gresse et al., 1992; Newton, 1993; Fig. 4a and b).

The longest of the fault arrays is the Kango Fault with a total length of 230 km from its western end at Ladismith to its eastern termination, southwest of Willowmore (Fig. 4a). The fault array comprises four discernible segments. The western segment of the fault is 70 km long (Location I, Fig. 4a) and consists of an E–W-trending single fault scarp of approximately 800 m relief that juxtaposes Silurian sequences in the footwall and Devonian sediments in the hangingwall. The western termination is evident from a splaying of the single fault into a number of smaller faults (Location II, Fig. 4a). To the east, the E–W-trending fault has a right-step in trend (Location III) with Pre-Cape strata in its footwall and a dissected W plunging anticline in its footwall. This geometry is similar to that of a hard linked boundary between two fault segments (e.g. Trudgill and Cartwright, 1994). The central segment of the Kango Fault (Location IV, Fig. 4a) has no significant topographic expression and is evident from the juxtaposition of the Pre-Cape Group or Table Mountain Group strata in its footwall with Mesozoic sediments of the Oudtshoorn Basin in its hangingwall (Barnett et al., 1997). This central segment, which is 100 km long, has an E–W trend and its western extent is defined by a minor change in trend from 090° to 100° at Stomptdrift (Location V, Figs. 4a and 5a-i). This change in trend is co-incident with an intra-basin high in the hangingwall that is composed of pre-rift strata and separates two Mesozoic depocentres. Along the majority of the trend of the fault syn-rift strata dip into the fault (Fig. 5a-iii); however, at this intra-basin high the strata dip parallel to the fault and onlap onto the high (Fig. 5a-ii). The hangingwall pre-rift outcrop, therefore, corresponds to a paleo-segment boundary.

To the east of the Stomptdrift intra-basin high (Location V), two shorter segments are discernible. These two segments correspond with the occurrence of Mesozoic strata within the hangingwall (Locations VI and VIII, Figs. 4a and 5a-i) separated by an intra-basin high comprising Devonian strata at Geelboslaagte (Location VII, Figs. 4a and 5a-i). The first of the two segments (Location VI) trends 100° and juxtaposes the Table Mountain Group pre-rift strata against syn-rift sediments with a well-defined fault scarp (approximately 100 m relief). The 20 km length of this segment is defined as the distance from the centre of the Stomptdrift intra-basin high (Location V) to the centre of the Geelboslaagte intra-basin high (Location VII). The second segment (Location VIII, Figs. 4a and 5a-i) is also 20 km long; however, unlike the other segments, it has a curvilinear fault trend (Fig. 5a-i) that is parallel to the trend of the pre-rift strata in the immediate footwall. The Kango Fault array, therefore, comprises five discernible segments that have lengths (from west to east) of 70, 100, 30, 20 and 20 km that have a co-linear trend relationship.

On a regional scale, the Kango and Baviaanskloof faults have an en-échelon, right stepping relationship, corresponding to a non-breached relay ramp (Location IX, Fig. 4).

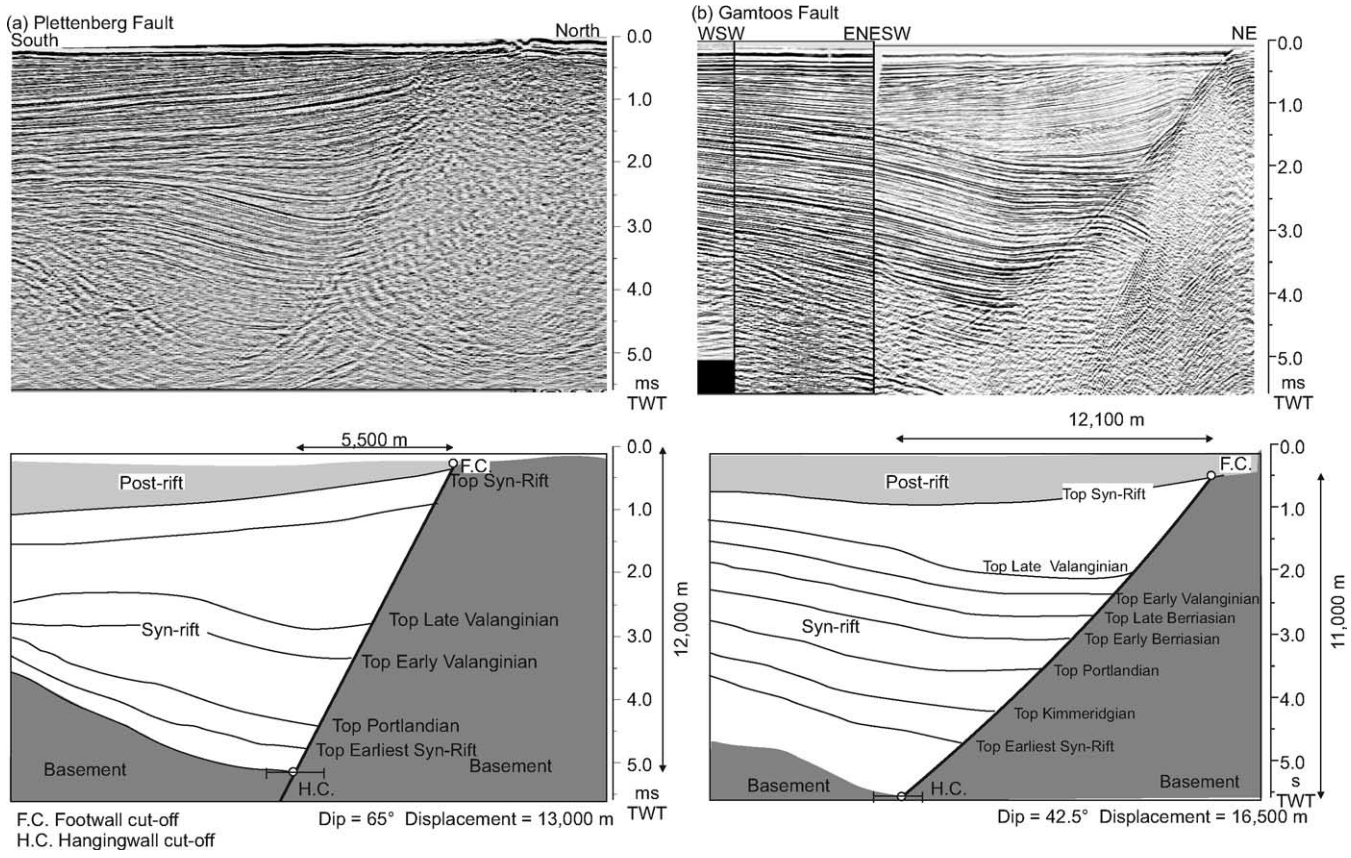

Fig. 7. Seismic sections (interpreted and uninterpreted) across the Plettenberg and Gamtoos (offshore) faults that demonstrated the planar geometry of both faults to a depth of at least 11,000 m. In each section the mapped horizons, the position of hangingwall and footwall cut-offs, and the true-depth of the section (in metres) have been plotted. Mapped horizons have been correlated and age determined from the 27 available exploration wells (Fig. 6). The true depth is then used to calculate displacement and dip.

The Baviaanskloof Fault array, with a total length of 80 km, has a continuous scarp and a linear trend and step free fault trend. Despite the linear nature of the fault trend, the hangingwall comprises two isolated Mesozoic depocentres (Locations X and XII, Figs. 4a and 5b) separated by Silurian Kouga pre-rift strata (Location XI). It is, therefore, interpreted that this portion of the fault system comprises two linked fault segments that are 25 and 45 km long (west and east, respectively), although the continuous fault scarp indicates that the fault has linked across, and breached, the intra-basin high. The eastern end of the 45-km-long segment is defined by an abrupt change in trend from 075° to 090° (Location XIII, Fig. 4a), which also demarcates the western end of the third segment. This third segment, which is 10 km long, has no Mesozoic depocentres preserved in its hangingwall and juxtaposes Ordovician against Devonian strata. The eastern tip dies out within the Ordovician Peninsula Formation (Location XIV, Fig. 4a).

As with the area between the Kango and Baviaanskloof faults (Location IX, Fig. 4), there is a right-stepping en-échelon configuration between the Baviaanskloof and Gamtoos faults (Location XIV, Fig. 4a).

The onshore portion of the Gamtoos Basin has been extensively studied by Shone et al. (1990) and Booth and Shone (1992). It comprises a complex cropping out of Mesozoic, Cape Supergroup and Pre-Cape strata (Fig. 4a).

At all locations the contacts between the three units are fault-bound with the Gamtoos fault containing Mesozoic, syn-rift strata in its hangingwall and Pre-Cape strata in its footwall, while the Elandsberg Fault has Pre-Cape as its footwall and Table Mountain Group in its hangingwall generating a Gamtoos horst structure. Shone et al. (1990) argue that the Pre-Cape group has undergone multiple phases of deformation; they note, however, that the most prominent deformation fabric is associated with the Cape Orogeny. These older structures have the same trend as the Gamtoos Fault (Fig. 4b), and the Gamtoos Fault is considered to have reactivated a Cape Fold Belt fault. At approximately 30 km from the western tip of the Gamtoos Fault (Location XV, Fig. 4a), there is a SW–NE-trending fault that links the Gamtoos and Elandsberg faults. The Gamtoos Fault continues to the SW where it is not exposed because of Quaternary deposition, although its trace can be directly linked to that of the offshore fault. The total length of the onshore Gamtoos Fault is 80 km.

In the offshore area the Plettenberg and offshore continuation of the Gamtoos faults were investigated (Fig. 6). Although there is no bathymetric expression of either the Plettenburg or Gamtoos fault planes, the faults are imaged in the seismic data and their surface projections are derived from the position of hangingwall and footwall cut-offs (Figs. 6 and 7). The seismic data are 2D and as the fault planes were mapped in sections both perpendicular

and parallel to the fault trace, by interpolating TWT fault picks, 3D fault geometries were established.

The Pletmos and Gamtoos basins have similar geometries. They are half-grabens that exhibit a change in trend from approximately WNW–ESE to N–S in the east of the basins, and their basin-bounding faults down-throw towards the south or southwest (Bate and Malan, 1992; McMillan et al., 1997). The two basin-bounding faults have trends that are identical to that of the immediately adjacent onshore basement pre-rift fabric (Figs. 4 and 6 for comparison). The Plettenberg Fault is likely to be associated with the localised onshore Mesozoic exposure at Plettenbergbaai (Fig. 6a). The offshore Gamtoos Fault is a direct continuation of the onshore portion. As a consequence of the absence of data in the southeast margin of the two basins, the total length of the faults cannot be established; however, the faults have minimum lengths of 160 and 170 km (Plettenburg and onshore and offshore Gamtoos, respectively). Later discussion will refer to the observed, and hence minimum, fault length.

Despite the change in trend of both of the faults from a WNW–ESE to a N–S orientation (Fig. 6), the cross-sectional geometry of the faults remains the same along the entire length of the faults (Fig. 8). Interpolation of the fault plane to form a 3D surface produces fault planes that are discrete, approximately continuous, smooth surfaces without steps in trend (Fig. 8). In addition, there is no evidence of abandoned fault tips in either the hangingwall or footwall, or an en-échelon configuration and, therefore, the faults do not comprise non-linear fault segments.

The principal limitation in determining the plan view geometry of the offshore bounding faults is that of line spacing ($\sim$500 m in the NE of the fault and $\sim$5 km in the north and southeast), although in all sections there is only one fault plane visible. Therefore, if the faults were segmented with an en-échelon configuration, the region of overlap (where the trace of two faults would be expected) would have to be contained entirely within the area between two seismic sections. Given that the displacement is consistently $>$12 km, to explain the

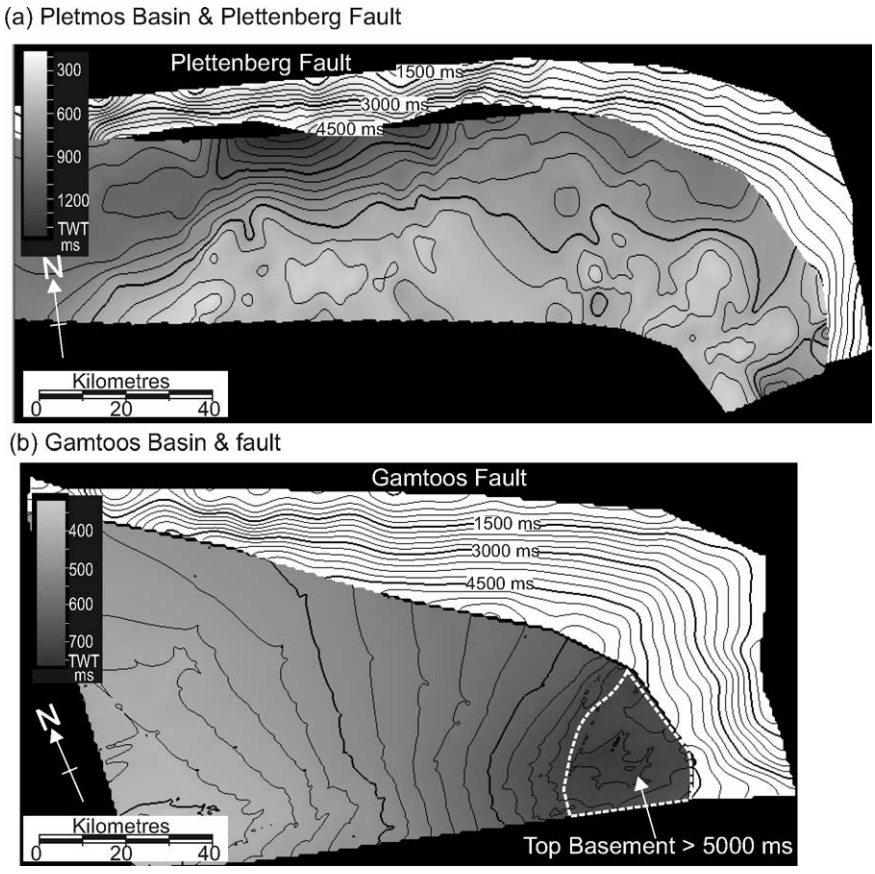

Fig. 8. Contoured plots of (a) Pletmos Basin and Plettenberg Fault and (b) Gamtoos Basin and fault. In both plots, fault planes are shown in white with black contours and correspond to two-way-travel-time (TWT, in ms) to the observed fault plane (Fig. 7) that uniformly dip towards the south or southwest. These plots demonstrate the continuous, linear and non-segmented nature of both fault planes suggesting that they are not comprised of multiple, en-échelon configured segments (see text for discussion). The grey-shaded areas in both plots are contoured plots of the thickness (in TWT, ms) of the earliest resolvable syn-rift sequences; light shading corresponding to areas of thinner sequences and dark shading to thicker sequences. In both basins the sequences thicken significantly into the bounding faults with the location of maximum accumulation occurring in the west for the Plettenberg fault and the southeast for the Gamtoos fault. The sequences are continuous across the entire basin and there is no evidence of any isolated depocentres or intra-basin highs. Furthermore, the only faults observed are the basin bounding faults; no intra-basin faults are observed. (The shaded plot for the Pletmos Basin corresponds to TWT thickness of Top Portlandian to Top Early Syn-Rift while the shaded plot for the Gamtoos Basins corresponds to TWT thickness of Top Early Syn-Rift to Top Basement. In the deepest portion of the Gamtoos Basin (southeast) the Top Basement reflection is below the maximum recording time of 5000 ms, therefore true thickness of the sequence is uncertain.)

occurrence of only one fault plane one would have to invoke either extreme fault tip gradients (from 12 km to displacement less than ~50 m seismic resolution within <5 km) or transfer faults that are co-incident with the area between sections. The former is unrealistic and the latter can be ruled out from sections that are parallel to the bounding fault trace.

2.1.2. Cross-section and displacement

The Kango and Bavainskloof Fault planes are visible at some localities and dip at approximately 60° towards the south (Fig. 5a and b); the sub-surface dip is unconstrained, although some workers have suggested that it may become more shallow at depth (de Wit and Ransome, 1992). The onshore Gamtoos fault plane is not visible. In addition, at a number of localities the Kango Fault juxtaposes syn-rift intervals against the basement with the syn-rift sequence diverging towards the fault (Fig. 5a-iii). However, the depth to the top pre-rift sequence and the amount of footwall erosion for the onshore faults is unknown so. It is, therefore, impossible to determine displacement. Even where the pre-rift crops out in the hangingwall it is not the same sequence as in the corresponding footwall and, therefore, cannot be used to quantify displacement.

In contrast, using the available sub-surface data it is possible to determine both cross-sectional geometry and displacement for the offshore faults. This requires: (1) identification of hangingwall and footwall cut-offs; (2) depth conversion of sections; and (3) determination of displacement.

2.1.2.1. Identification of hangingwall and footwall cut offs. As discussed, the location of both the Plettenberg and offshore Gamtoos fault planes are well imaged (Fig. 7). In the middle and lower sections the resolution is reduced by diffraction (a consequence of incomplete migration) and occasional refraction of syn-rift reflection ray paths through the fault plane, resulting in less well constrained fault planes for determining the positions of the hangingwall cut-off. The interpreted hangingwall is shown on the seismic sections with an estimate of the error. Using the location of hangingwall and footwall cut-offs, the heave (i.e. horizontal offset) on the faults is calculated to be 5500 m for the Plettenberg and 12,100 m for the Gamtoos. The errors in determining the heave as a consequence of seismic resolution are considered to be negligible for the hangingwall cut-off and are estimated to be approximately 100–200 m (~1–2%, Fig. 6) for footwall cut-offs.

2.1.2.2. Depth conversion and displacement determination. Previous studies have compiled time–depth conversion functions for the two basins (McMillan et al., 1997; Paton, 2002). Using this function, the depth of the fault cut-offs are converted from TWT (ms) to depth (m) and the throws on the two faults using the sections are calculated to be 12,000 m for the Plettenberg Fault and 11,000 m for the Gamtoos Fault. The displacements of the hangingwall to footwall cut-offs are estimated to be 13,000 m and 16,500 m for the Plettenberg and Gamtoos Faults with dips of 65° and 43°, respectively.

As this is the displacement between hangingwall and footwall cut-offs, to estimate true displacement the following factors have to be considered: amount of flank uplift and footwall erosion; the degree of preservation of hangingwall sequences; sediment compaction; the balance between sediment supply and accommodation space creation; and eustacy.

To establish the total cumulative displacement of the fault the key uncertainties are the magnitude of flank uplift and erosion, effect of post-rift compaction on sediment fill and water depth of the basin.

Ideally, the syn-rift interval would be preserved on both hangingwall and footwall sides of the fault and, therefore, true displacement would be easily determined. Unfortunately, the footwalls to both faults in the sections with greatest displacement are sub-aerially exposed, resulting in two sources of error. First is the thickness of any footwall syn-rift interval that has subsequently been eroded and second is the magnitude of flank uplift (e.g. Anders et al., 1993). For the Plettenberg Fault, although the section that contains the greatest displacement (Fig. 6a) has no syn-rift sequence on its footwall, sections at the eastern margin of the basin show a very thin (~100 ms) footwall syn-rift interval (McMillan et al., 1997; Paton, 2002). Furthermore, in these sections there is no evidence of flank uplift. Even if these observations do not apply to the section of interest in this study, the displacement determined can be considered as a minimum estimate for the true displacement. The Gamtoos Fault may have up to 500 m of footwall erosion (Paton and Underhill, 2004); however, as with the Plettenberg Fault, the displacement derived in this study is a minimum estimate of true displacement.

A further source of error is erosion within the hangingwall sequences; however, in both basins, seismic interpretation, coupled with the extensive well data, reveals only minor unconformities and near continuous deposition having occurred. Compaction of sediments would also have the effect of reducing the observed displacement, although to estimate the final displacement only compaction associated with post-rift deposition is important. Any compaction will result in an underestimate of final displacement. Water depth must also be considered, although only the water depth at the syn-rift to post-rift transition is important for the final displacement calculation. The final syn-rift sequences are continental shelf deposits and water depths may have been up to a maximum of 150 m (McMillan et al., 1997). However, as this water depth only corresponds to 0.7% of the estimated total displacement, it is considered negligible and, therefore, can be ignored.

Given these considerations, where the uncertainty cannot be quantified, or even qualitatively estimated, this study has used a method that has consistently underestimated the true final displacement on both faults. The calculated cumulative displacements, therefore, of 13,000 and 16,500 m for the Plettenberg and Gamtoos Faults may be considered to be conservative estimates.

2.2. Basin fill evolution as a proxy for fault evolution

An important consideration in using syn-rift sediment accumulation as a proxy for tectonically controlled accommodation space and fault activity (e.g. Anders and Schlische,

1994; Morley, 1999; Dawers and Underhill, 2000; Contreras et al., 2000; McLeod et al., 2000), is the balance between sediment supply and accommodation space creation. As this balance is very different between the onshore and offshore portions of the South African extensional systems, their evolutions have to be considered separately.

2.2.1. Evolution of onshore basin bounding faults

The sedimentology of the onshore syn-rift interval predominantly comprises non-marine conglomerates and sandstones (Fig. 5a and b; McLachlan and McMillan, 1976; Dingle et al., 1983). The intra-basin highs and associated isolated Mesozoic depocentres in the onshore basins suggest that at some stage during the early syn-rift interval the fault arrays comprised a number of isolated segments. The present day configuration of fault scarps that are continuous across both pre-rift exposures (intra-basin highs) and syn-rift depocentres (e.g. Fig. 5b-iii) suggests that the later syn-rift intervals were controlled by throughgoing fault systems that had more extensive, continuous depocentres that have subsequently been eroded in places to reveal the earlier isolated depocentres (Fig. 5b-ii). This conjecture is supported by sedimentological and paleontological correlations along the fault system that demonstrate that the late syn rift interval, which now occurs in isolated deposits, formed a more continuous depocentre (Fig. 9a; McLachlan and McMillan, 1976; Dingle et al., 1983). However, given the absence of either detailed timing constraints or along-fault accumulation variation data, it is difficult to constrain the development of the onshore faults further.

2.2.2. Evolution of offshore basin bounding faults

In contrast to the onshore portion, facies and paleontological studies demonstrate that the Pletmos and offshore Gamtoos basins were under-filled for the majority of the syn-rift interval (Bate and Malan, 1992; McMillan et al., 1997; Paton and Underhill, 2004). Given this under-filled nature, it is anticipated that sediment would be preferentially deposited into fault controlled depocentres and, therefore, areas between active depocentres would have very little, if any, sediment accumulation (Fig. 9b). As the thickness of each seismic package in this data set is significantly greater than seismic resolution (~200–400 ms compared with ~50 ms), the number of isolated depocentres in an under-filled basin is equivalent to the number of fault segments (compare Fig. 9b and c). Plotting sediment accumulation versus length in a transect parallel to the trend of the faults reveals the presence, or absence, of isolated depocentres. From such a fault parallel plot, the fault evolution can be inferred (e.g. McLeod et al., 2000).

In this study it is possible to investigate the sediment accumulation at two sampling resolutions (Fig. 10). The first is at a basin scale using 2D sections that are perpendicular to fault trace and intersect the location of maximum sediment accumulation. The sampling resolution, determined by the frequency with which the 2D sections intersect the fault plane, is approximately 5 km in the west and 500 m in the northeast (Fig. 10). In parts of the two basins the Top Basement reflection occurs at a TWT that is deeper than the maximum recording time of the sections and, therefore, accumulation has been calculated from the earliest syn-rift reflection mappable across the entire basin to sequential syn-rift horizons.

The second is at a significantly higher sampling resolution and is derived for at least part of the fault trace where the trend of a 2D section is co-incident with, and parallel to, the location of maximum sediment accumulation. In these sections sediment accumulation was sampled at 150 m spacing over a distance of 30 and 32 km for the Plettenberg and Gamtoos

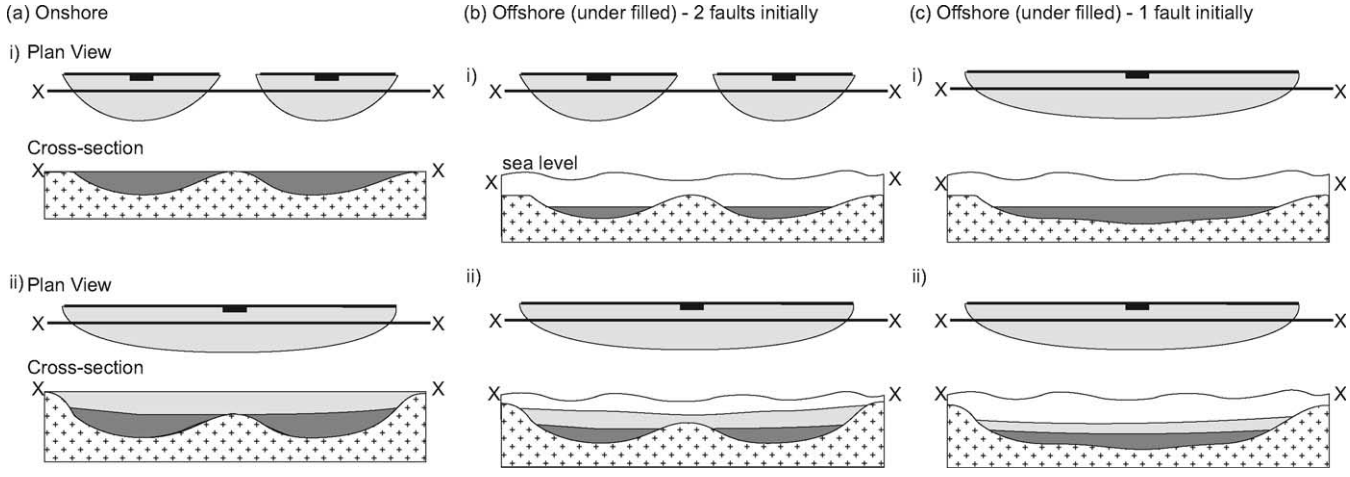

Fig. 9. (a) Schematic diagram to illustrate the development of the onshore faults where sediment supply is equal to tectonic accommodation space creation. Initially (i) there are two separate but co-linear fault segments with associated isolated depocentres (dark grey fill). Subsequently (ii) the co-linear segments coalesce to form a single depocentre (light grey fill). (b) and (c) Cartoon of the development of the offshore faults where sediment supply is less than tectonic accommodation space creation. Two scenarios are presented. (b) Two co-linear isolated faults, each with a discernable, isolated depocentre that remains under filled link to form a single throughgoing fault; this scenario has a persistent intra-basin high. This will be resolvable if the thickness of the early depocentres is greater than seismic resolution. (c) A single fault with depocentre increases in displacement through time. In the offshore South Africa data only a single depocentre is evident, although it is likely that scenario (b) is applicable with the isolated depocentre stage occurring very early in the rift episiode and beyond seismic resolution; see discussion (after Schlische and Anders, 1996).

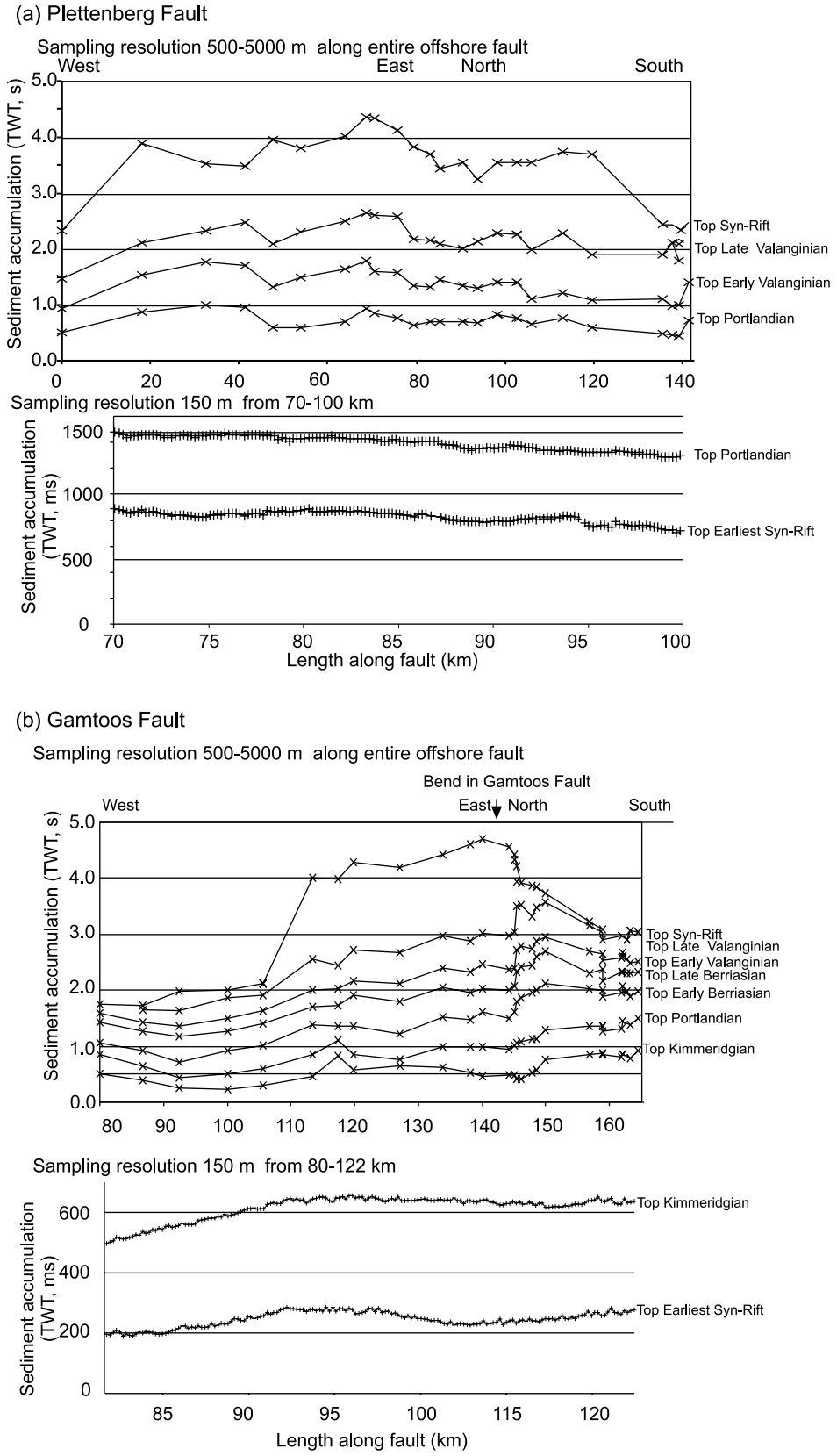

Fig. 10. Preserved sediment accumulation vs. length along fault for (a) Plettenberg Fault and (b) Gamtoos Fault. As discussed in the text, two horizontal sampling resolutions were undertaken for both basins with (i) corresponding to low resolution (500–5000 m) along the entire length of the faults, and (ii) corresponding to high resolution (150 m) along a portion of the fault. Given the data constraints discussed in the text, the low resolution data corresponds to accumulation from Top Early Syn-Rift horizon to subsequent horizons while the high resolution data corresponds to accumulation from Top Basement horizon to subsequent horizons. In each basin the observed syn-rift intervals are continuous along the entire lengths of the faults with no evidence of isolated depocentres or intra-basin highs. This is particularly evident in the high resolution data.

Faults, respectively. In both of the high resolution sections the Top Basement reflection is evident and, therefore, the sediment accumulation plots correspond with Top Basement to Top Earliest Syn-Rift and Top Basement to Top Kimmeridgian (Plettenberg and Gamtoos basins, respectively). A limitation of the available data is that the seismic coverage does not include the fault tips. The western tips of both faults are evident onshore (Fig. 4); however, in neither basin is the eastern tip evident from available data. The fault lengths are therefore a minimum, and an understanding of how the fault has evolved can only be determined for the observed length.

At both sampling resolutions the syn-rift intervals are mappable along the length of the faults and at no position on either fault profile does sediment accumulation reduce to zero. There is no evidence of variations in sediment accumulation on the high resolution sampling and only minor variations in the low sampling resolution. Given the low amplitude, long wavelength variations in the latter, and that it is observed across all of the sequences, these variations are considered to be associated with minor changes in sediment dispersal patterns and accumulation, rather than being fault controlled. There is, therefore, no evidence for individual depocentres along the observed portions of either fault and, hence, the observed current lengths of the faults have been established by the deposition of the earliest resolvable syn-rift sequences. This is supported by seismic sections parallel to the faults (Fig. 11) in which there is no evidence of intra-basin depocentres and syn-rift intervals progressively thin towards the western tips of the faults (the eastern tips are out with the data area). The development of the western portions of the fault beyond the seismic coverage is unconstrained.

The observation that the offshore faults are comprised of single segments, at the resolution and extent of the data, is therefore contrary to the observed onshore faults that were comprised of co-linear, but isolated, segments during the early syn-rift episode. Given the continuity in the Cape Fold Belt fabric across the study area, it is likely that the offshore faults would have evolved in a similar way to the onshore faults and co-linear segmentation in the early syn-rift would be expected. As there is no evidence even within the high resolution data (Fig. 10), any depocentres must either be thinner than the vertical resolution (~50 m) or segments are longer than the 30 km extent of the high resolution data.

2.2.3. Growth trends of Plettenberg and Gamtoos Faults through time

Using the sediment accumulation plots for the Plettenberg and Gamtoos Faults, combined with age constraints (Gradstein et al., 2004), the temporal change in fault length and displacement can be determined, although given the unconstrained western fault tip some caution must be used.

As each package is continuous within the seismic coverage (100 km for Gamtoos and 160 km for the Plettenberg faults), the minimum fault length versus cumulative displacement for each sequence can be calculated (i.e. from Top Basement to sequential syn-rift intervals; Fig. 12). Two error bars are included on the plot to account for the uncertainty in fault tip position. The first error bar accounts for the eastern tip exposed onshore and gives the length of the fault as the observable length plus the length of the onshore portion. The extent of the fault to the west is unconstrained; however, as it is a log–log

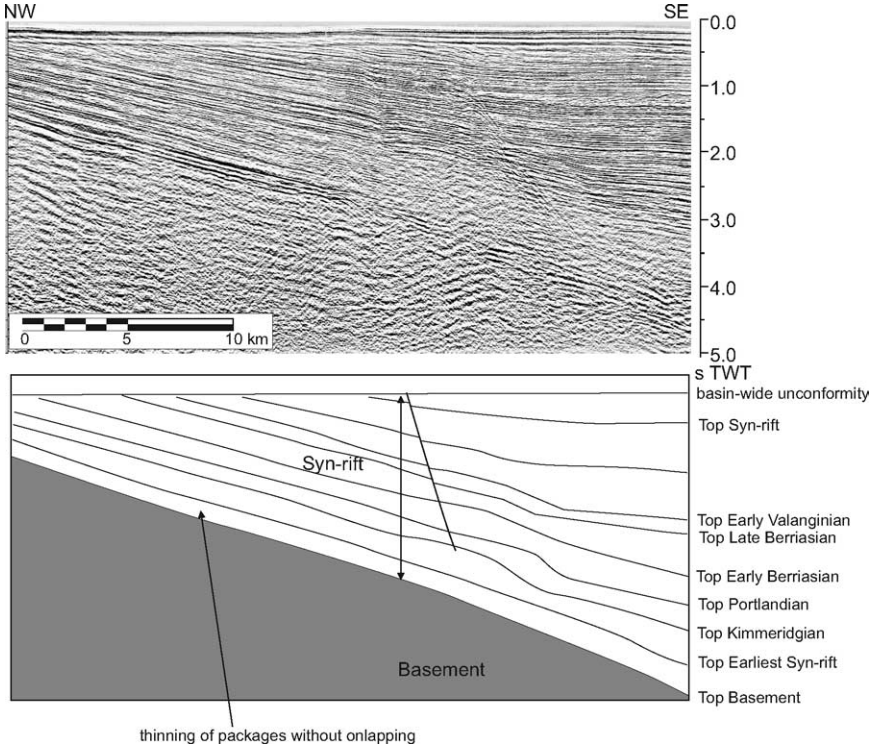

Fig. 11. Seismic section (and interpretation) parallel to, and in the immediate hangingwall of, the Gamtoos Fault (Fig. 6 for location). This section demonstrates the gradual thinning of even the earliest syn-rift intervals towards the NW without evidence of isolated depocentres or intra-basin faults being present.

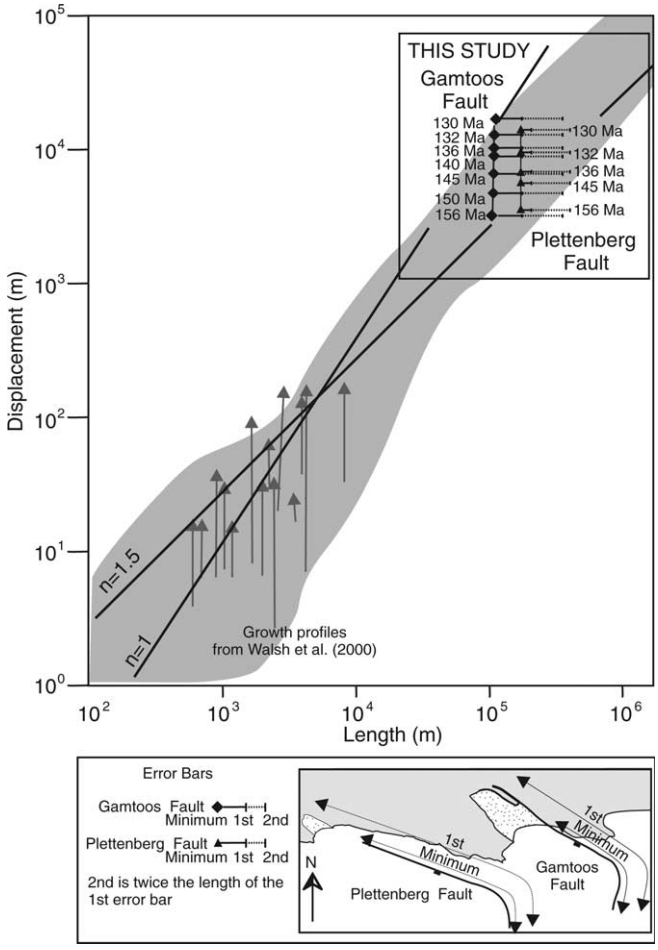

Fig. 12. Displacement vs. length (D–L) plot for the Plettenberg and Gamtoos Faults with the calculated D–L value for each age plotted. This demonstrates the near vertical nature of the growth path, corresponding to early establishment of length prior to accruing displacement. The fault growth paths of Walsh et al. (2000) have also been plotted and demonstrate that despite the dimensions of the South African faults being two orders of magnitude greater than those of the Walsh et al. (2000) study, the growth paths are very similar. As discussed in the text, the final lengths of the faults are not observed within the data area. To account for this uncertainty in length, for each sequence three fault lengths are plotted (insert shows how the three lengths were derived). The minimum length corresponds to that observed using seismic data alone; the first error bar corresponds to the entire length of the observed fault (both onshore and offshore) and the second error bar considers the scenario in which only half the entire fault length is observable; see text for discussion. The grey shading corresponds to data of Schlische et al. (1996) and n corresponds to the constant in the scalar relationship $D = cL^n$.

plot even if we assume that we are only observing a portion of the total fault length, for instance 50%, which would give an unrealistically long 400 km single fault, there is little variation in data spread (revealed by the second series of error bars in Fig. 12).

Regardless of which error bars are used, each fault has a near vertical growth trend because the sequences have similar lengths and only accrue displacement through time.

2.2.4. Intra-basin fault development

The development of the intra-basin setting was investigated by constructing isochron plots (Fig. 8) for the earliest syn-rift interval (Top Basement to Top Early Syn-Rift). The isochron plots demonstrate that during this interval, sediment accumulation was entirely controlled by the basin-bonding fault. There is no evidence for isolated depocentres across the basin and the only thickening of the package is into the basin-bounding fault; no intra-basin faults were active during the earliest resolvable syn-rift interval.

3. Model for the evolution of the South African fault system

The observations presented in this study are used to develop a model for the evolution of the fault system (Fig. 13) that has many similarities to the model proposed by Walsh et al. (2002); this will be discussed later. The pre-rift heterogeneity comprises the Cape Fold Belt structural fabric, which is dominated by S-dipping, E–W- and NE–SW-trending compressional faults (Fig. 13i). With subsequent Mesozoic extension, the pre-existing reverse faults are used as seed-points for the new extensional faults. A series of co-linear isolated extensional faults and corresponding depocentres are established. With continued extension, the presence of the pre-existing fault results in the rapid radial growth of faults tips without the inhibition of rupture barriers along the reactivated reverse fault plane. The isolated depocentres rapidly coalesce as a very long, under-displaced normal fault forms. A consequence of the rapid strain localisation onto the pre-existing faults at an early stage results in the absence of intra-basin faults. Subsequent extension is accommodated through an increase in fault displacement.

4. Discussion

Previous studies have documented that the extensional system of southern South Africa was formed through the negative structural inversion of the Cape Fold Belt and that the pre-existing reverse faults controlled the location and trend of the Mesozoic normal fault arrays (Section 1.2). It is, therefore, possible to evaluate the influence of the Cape Fold Belt structural fabric on the development of the extensional system both in terms of fault length–displacement, and in the context of established fault growth models.

4.1. Influence of pre-existing structures on segment configuration, cumulative length and displacement

The extensional system of southern South Africa comprises fault arrays that have lengths of 230 km (Kango), 80 km (Baviaanskloof), >170 km (onshore and offshore Gamtoos) and >160 km (Plettenberg). Given that the Kango, Baviaanskloof and Gamtoos arrays are along trend of each other, and areas of overlap between the arrays are characteristic of transfer zones, they can be considered part of the same fault system that is at least 480 km long. The fault system, and the arrays that comprise it, are therefore comparable with the longest fault systems that have been documented in continental lithosphere (e.g. Basin and Range, northeast US, East Africa; Machette et al., 1991; Schlische, 1992; Anders et al., 1993; Schlische and

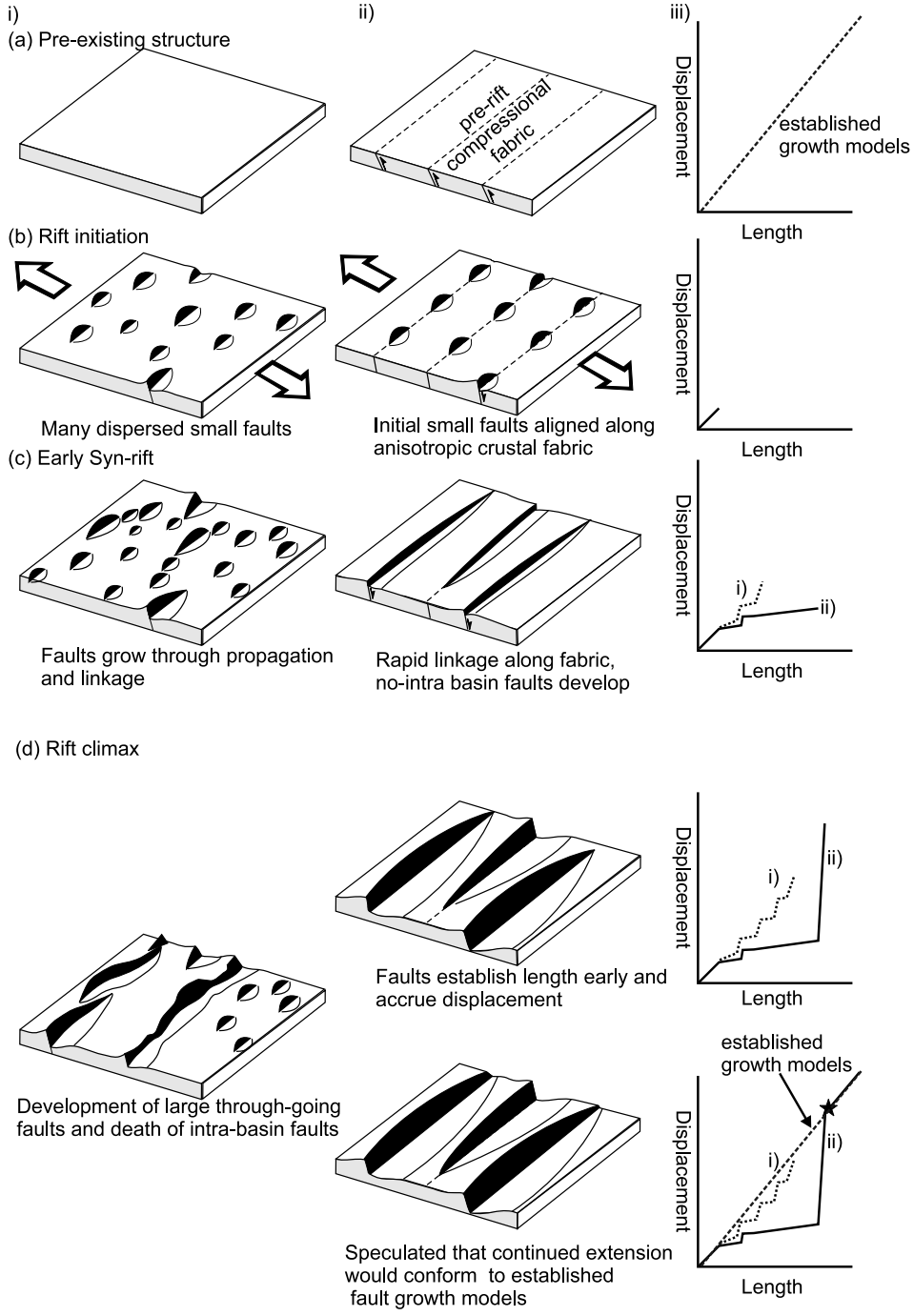

Fig. 13. Comparison of the growth of normal faults in settings with (i) no pre-existing structure in cases (i) and (ii) and the location of the pre-existing compressional fault for case (ii). Figure (iii) represents the development of schematic D–L relationships during the rifting process. (a) Pre-extensional configuration. (b) Rift initiation is dominated in (i) by many short, low displacement and dispersed faults, while in (ii) small, isolated faults are aligned along the crustal fabric. (c) During the early stage of rifting the faults in (i) grow through lateral propagation and linkage, commonly forming en-échelon configurations, while in (ii) rapid linkage occurs along the fabric with no development of intra-basin faults. This is reflected in the variation in growth paths in (iii). (d) At rift climax established fault growth models (i) predict the development of long, throughgoing, large displacement faults, with the death of intra-basin faults. In (ii) the faults established their length previously and only accrue displacement resulting in the near vertical growth path (iii). Case (i) also differs from (ii) with respect to displacement rate because in (i) as strain is progressively localised, displacement rate of the bounding fault increases, while in (ii) as strain is localised, the very early displacement rate remains approximately constant. (e) It is conjectured that in the extensional system of southern South Africa the intersect (shown by the star) of the growth profile in model (ii) and established fault growth models may be controlled by the pre-existing compressional fault that is reactivated. It is predicted that had extension continued in South Africa the faults would have altered their growth path and would subsequently have followed the predicted path. To test this conjecture, studies in other regions of negative structural inversion will have to be undertaken (after Cowie et al., 2000; Walsh et al., 2002).

Anders, 1996; Ebinger et al., 1999; Morley, 1999; Contreras et al., 2000). Where the South African fault system differs from these previously documented faults systems is that the latter have plan view geometries characterised by en-échelon and stepped fault traces at a variety of scales from ~ <5 km up to ~100 km, with the change in fault trace attributed to the coalescing of fault segments. The faults in this study do not show this style of en-échelon segmentation with linear traces of up to 100 km (e.g. Kango Fault; Fig. 4). However, from the onshore evidence, the presence of intra-basin highs and isolated depocentres (e.g. western Baviaanskloof; Location XI, Fig. 4a) suggest that the early syn-rift episode comprised a number of co-linear, but isolated depocentres, which, during continued extension, coalesced to form longer and more continuous depocentres. As this difference is considered to be an effect of the pre-existing Cape Fold Belt fabric, the model for the evolution of the South African extensional faults is characterised by the presence of co-linear fault segments during the early rift episode (Fig. 13a).

The large cumulative displacement and long length of the South African faults, which are minimum estimates given the unconstrained location of the western fault tips, raise the issue of how such large, brittle structures can be supported within the lithosphere. A key factor in determining the final dimensions of extensional faults is considered to be the effective elastic thickness of the lithosphere (Forsyth, 1992; Buck et al., 1999). Jackson and White (1989) observed that a common maximum fault segment length of 25 km long is consistent with that of a typical thickness for continental lithosphere.

The elastic thickness of the study area is unknown, although Harvey et al. (2001) have estimated a crustal thickness of 36–44 km from seismic receiver functions for the southwestern region of South Africa; as this is in an equivalent position along trend of the study area, it is reasonable to assume a similar crustal thickness in the study area. The occurrence of a thickened continental lithosphere, and hence a larger elastic thickness, has been used to explain other examples of atypically large extensional systems (e.g. East Africa and Baikal rifts), although additional factors such as rheological variations and low geothermal variations may also be important (Foster and Nimmo, 1996; Jackson and Blenkinsop, 1997; Ebinger et al., 1999; Buck et al., 1999). A further complication is the poorly constrained nature of the lithosphere beneath the Cape Fold Belt (Harvey et al., 2001) and what its role may be in influencing the strength of the lithosphere of the study area. However, what is evident is that the lithosphere of South Africa is strong enough to accommodate high angle (40–60°), brittle structures that have displacements of up to 16 km.

4.2. Influence of pre-existing structure on fault system evolution

Given the well constrained nature of the pre-existing Cape Fold Belt fabric, it is possible to test the validity of established fault growth models (e.g. Cowie et al., 2000) on a crustal scale fault system within a region of significant crustal heterogeneity (Fig. 13). In particular: (a) the temporal displacement–length (D–L) relationship of the bounding faults; and (b) partitioning of strain between the bounding fault and faults within the half-graben can be addressed.

4.2.1. Do faults grow in accordance with D–L scaling relationship?

The description of D–L scaling in terms of a power law relationship (e.g. Walsh and Watterson, 1988; Cowie and Scholz, 1992; Gillespie et al., 1992; Dawers et al., 1993) only considers the final cumulative displacement and length; there is little or no consideration for the development of the scaling relationship through the evolution of the fault system. Recently there has been increased focus on how an individual fault array, or system, evolves through time. Bellahsen et al. (2003) observed that small-scale faults did not necessarily evolve according to a power-law relationship and discussed that the gradient of the regression line in the D–L plot was influenced by rheology, extension velocity and layer thickness.

On a basin scale, Morley (1999) demonstrated that the growth of some faults in the East African Rift rapidly established their length during the early syn-rift episode prior to accumulating displacement and hence had steep D–L profiles. Walsh et al. (2002) quantified a similar observation in their study in East Timor and documented the near vertical D–L growth profile of individual faults (Fig. 12). Their study investigated faults with lengths of up to 8 km and displacements of 170 m. The near vertical growth trend of the South African faults documented in this study is in agreement with the conclusions of Walsh et al. (2002) and furthermore demonstrate that faults can establish lengths of at least 160 km within <6 Myrs after rift initiation, or <20% rift duration, if there is a significant pre-existing fabric.

The occurrence of near vertical growth trends in D–L growth profiles raises the question of why, in both the examples of Walsh et al. (2002) and the South African faults presented here, do the final D–L values plot in accordance with established D–L relationships with a scaling exponent of between $n=1$ and $n=1.5$ (Fig. 13). Given that in both cases the observed faults are reactivating pre-existing faults, it is possible to speculate that the later extensional faults may be inheriting the final D–L values of the underlying faults (Fig. 13c). To validate such speculation would require a better understanding of the pre-extensional deformation; in the case of South Africa, the D–L profile of faults controlling the Cape Fold Belt. From a mechanical viewpoint this makes sense as the extensional fault tips would rapidly propagate using the pre-existing plane of weakness from the pre-existing compressional fault. Propagation would cease when rupture barriers are reached; this would likely be the tips of the reactivated surface. The controlling rupture barriers would then only be overcome once the D–L profile had achieved that of the predicted model. Further extension would be accommodated through both fault tip propagation and segment linkage (Fig. 13d-iii).

4.2.2. Rapid strain localisation onto bounding fault

A further prediction of established fault growth models is that strain is progressively localised onto a smaller population

of faults throughout the rift episode, with the result that many early intra-basin faults cease to be active (e.g. Gupta et al., 1998; McLeod et al., 2000; Ackermann et al., 2001; Fig. 13b). The development of the offshore Gamtoos and Pletmos basins demonstrate that at least at the resolution of the seismic data there is no evidence of intra-basin faults and that by the deposition of the first resolvable package (<6 Myrs after rift initiation, or <20% rift duration), displacement is accommodated entirely on the basin bounding faults. These observations suggest that strain was very rapidly localised onto the basin-bounding fault in contrast to dispersed strain that leads to the development of intra-basin faults in most other extensional settings. It is proposed that this rapid strain localisation is a consequence of the pre-existing fabric (Fig. 13).

5. Conclusions

The pre-existing Cape Fold Belt fabric has exerted a significant influence on the development of the Mesozoic South African extensional system. In particular:

1. the fault arrays are composed of a number of coalesced segments that have a linear, rather than en-échelon, trend;
2. the underlying, reactivated compressional fault system, probably in combination with lithospheric constrains such as elastic thickness and rheology, has resulted in very long fault arrays (>160 km) with high angle fault planes (45–60°) and large displacements (16 km);
3. near vertical D–L growth profiles are observed;
4. strain is rapidly localised onto the bounding faults resulting in an absence of intra-basin faults even during the earliest resolvable syn-rift episode.

This study represents one end member of structural inheritance, where the orientation of strain has resulted in extensional structures reactivating pre-existing reverse faults on a basin scale. It is proposed that in other settings, where a similar orientation of strain and heterogeneity occurs, a similar modification of fault development should be expected.

Acknowledgements

This project was funded by a Natural Environment Research Council (NERC) Industrial CASE studentship with partners CASP; CASP are also thanked for covering the cost of fieldwork. This work benefited from discussions with John Underhill, David Macdonald, Patience Cowie, Estelle Mortimer and Joe Cartwright. Nicholas Bellahsen and an anonymous reviewer are thanked for their comments and suggestions on the original manuscript. Pete McFadzean and Suzie Francis are thanked for field assisting. I also gratefully acknowledge Petroleum Agency South Africa for access to 2D seismic and well data and in particular David Broad and Ian McLachlan for facilitating data release and support of the project. The University of Edinburgh's seismic interpretation facilities, using Schlumberger GeoQuest IESX software, were funded by the Centre for Marine and Petroleum Technology, Esso, Norsk Hydro and Shell. Computing support was provided by James Jarvis and Chris Place.

References

Ackermann, R.V., Schlische, R.W., Withjack, M.O., 2001. The geometric and statistical evolution of normal fault systems; an experimental study of the effects of mechanical layer thickness on scaling laws. Journal of Structural Geology 11, 1803–1819.

Anders, M.H., Schlische, R.W., 1994. Overlapping faults, intra basin highs, and the growth of normal faults. Journal of Geology 102, 165–180.

Anders, M.H., Spiegelman, M., Rodgers, D.W., Hagstrum, J.T., 1993. The growth of fault-bounded tilt blocks. Tectonics 12, 1451–1459.

Barnett, W., Armstrong, R.A., de Wit, M.J., 1997. Stratigraphy of the upper Neoproterozoic Kango and lower Paleozoic Table Mountain groups of the Cape Fold Belt revisited. South African Journal of Geology 100, 237–250.

Bate, K.J., Malan, J.A., 1992. Tectonostratigraphic evolution of the Algoa, Gamtoos and Pletmos Basins, offshore South Africa. In: de Wit, M.J., Ransome, I.G.D. (Eds.), Inversion Tectonics of the Cape Fold Belt, Karoo and Cretaceous Basins of Southern Africa. Balkema, Rotterdam, pp. 61–73.

Bellahsen, N., Daniel, J.-M., Bollinger, L., Burov, E., 2003. Influence of viscous layers on the growth of normal faults; insights from experimental and numerical models. Journal of Structural Geology 25, 1471–1485.

Booth, P.W.K., 1996. The relationship between folding and thrusting in the Floriskaal Formation (upper Witteberg Group), Steytlerville, Eastern Cape. South African Journal of Geology 99 (3), 235–243.

Booth, P.W.K., Shone, R.W., 1992. The Laurie's Bay fault: a pre-Cape-Table Mountain Group contact west of Port Elizabeth. In: de Wit, M.J., Ransome, I.G.D. (Eds.), Inversion Tectonics of the Cape Fold Belt, Karoo and Cretaceous Basins of Southern Africa. Balkema, Rotterdam, pp. 211–216.

Booth, P.W.K., Shone, R.W., 1999. Complex thrusting at Uniondale, eastern sector of the Cape Fold Belt, Republic of South Africa: structural evidence for the need to revise lithostratigraphy. Journal of African Earth Sciences 29, 125–133.

Booth, P.W.K., Shone, R.W., 2002. A review of thrust faulting in the Eastern Cape Fold Belt, South Africa, and the implications for current lithostratigraphic interpretation of the Cape Supergroup. Journal of African Earth Sciences 34, 179–190.

Broquet, C.A.M., 1992. The sedimentary record of the Cape Supergroup; a review. In: de Wit, M.J., Ransome, I.G.D. (Eds.), Inversion Tectonics of the Cape Fold Belt, Karoo and Cretaceous Basins of Southern Africa. Balkema, Rotterdam, pp. 159–183.

Buck, W.R., Lavier, L.L., Poliakov, A.N.B., 1999. How to make a rift wide. Philosophical Transactions of the Royal Society: Mathematical, Physical and Engineering Sciences 357, 671–693.

Cartwright, J.A., Trudgill, B.D., Mansfield, C.S., 1995. Fault growth by segment linkage: an explanation for scatter in maximum displacement and trace length data from the Canyonlands Grabens of SE Utah. Journal of Structural Geology 17 (9), 1319–1326.

Catuneanu, O., Hancox, P.J., Rubidge, B.S., 1998. Reciprocal flexural behaviour and contrasting stratigraphies: a new basin development model for the Karoo retroarc foreland system, South Africa. Basin Research 10, 417–439.

Catuneanu, O., Wopfner, H., Eriksson, P.G., Cairncross, B., Rubidge, B.S., Smith, R.M.H., Hancox, P.J., 2005. The Karoo basins of south-central Africa. Journal of African Earth Sciences 43, 211–253.

Cloetingh, S., Lankreijer, A., de Wit, M.J., Martinez, I., 1992. Subsidence history analysis modelling of the Cape and Karoo Supergroups. In: de Wit, M.J., Ransome, I.G.D. (Eds.), Inversion Tectonics of the Cape Fold Belt, Karoo and Cretaceous Basins of Southern Africa. Balkema, Rotterdam, pp. 211–216.

Coetzee, D.S., 1983. The deformation style between Meiringspoort and Beaufort West. In: Söhnge, A.P.G., Hälbich, I.W. (Eds.), Geodynamics of the Cape Fold Belt. Special Publication of the Geological Society of South Africa 12, pp. 101–113.

Contreras, J., Anders, M.H., Scholz, C.H., 2000. Growth of a normal fault system: observations from the Lake Malawi basin of the East African Rift. Journal of Structural Geology 22, 159–168.

Cowie, P.A., Scholz, C.H., 1992a. Physical explanation for displacement–length relationship of faults using post-yield fracture mechanics model. Journal of Structural Geology 14, 1133–1148.

Cowie, P.A., Scholz, C.H., 1992b. Displacement–length scaling relationship for faults using a post-yield fracture mechanics model. Journal of Structural Geology 14, 1149–1156.

Cowie, P.A., Gupta, S., Dawers, N.H., 2000. Implications of fault array evolution for syn-rift depocentre development: insights from a numerical fault growth model. Basin Research 12, 241–261.

Dawers, N.H., Anders, M.H., 1995. Displacement–length scaling and fault linkage. Journal of Structural Geology 17, 607–614.

Dawers, N.H., Underhill, J.R., 2000. The role of fault interaction and linkage in controlling synrift stratigraphic sequences: Late Jurassic, Statfjord East Area, northern North Sea. Bulletin of the American Association of Petroleum Geologists 84, 45–64.

Dawers, N.H., Anders, M.H., Scholz, C.H., 1993. Growth of normal faults: displacement–length scaling. Geology 21, 1107–1110.

de Wit, M.J., Ransome, I.G.D., 1992. The Cape Fold Belt; a challenge for an integrated approach to inversion tectonics. In: de Wit, M.J., Ransome, I.G.D. (Eds.), Inversion Tectonics of the Cape Fold Belt, Karoo and Cretaceous Basins of Southern Africa. Balkema, Rotterdam, pp. 3–14.

Dingle, R.V., Siesser, W.G., Newton, A.R., 1983. Mesozoic and Tertiary Geology of Southern Africa. Balkema, Rotterdam. 375pp.

Ebinger, C.J., Jackson, J.A., Foster, A.N., Hayward, N.J., 1999. Extensional basin geometry and elastic lithosphere. Philosophical Transactions of the Royal Society London A357, 741–765.

Forsyth, D.W., 1992. Finite extension and low angle normal faulting. Geology 20, 27–30.

Fossen, H., Hesthammer, J., 1997. Geometric analysis and scaling relations of deformation bands in porous sandstone. Journal of Structural Geology 19, 1479–1493.

Foster, A., Nimmo, F., 1996. Comparison between the rift systems of East Africa, Earth and Beta Regio, Venus. Earth and Planetary Science Letters 143, 183–195.

Gillespie, P.A., Walsh, J.J., Watterson, J., 1992. Limitations of dimension and displacement data from single faults and consequences for data analysis and interpretation. Journal of Structural Geology 14, 1157–1172.

Gradstein, F.M., Ogg, J.G., Smith, A.G., Agterberg, F.P., Bleeker, W., Cooper, R.A., Davydov, V., Gibbard, P., Hinnov, L., House, M.R., Lourens, L., Luterbacher, H.-P., McArthur, J., Melchin, M.J., Robb, L.J., Shergold, J., Villeneuve, M., Wardlaw, B.R., Ali, J., Brinkhuis, H., Hilgen, F.J., Hooker, J., Howarth, R.J., Knoll, A.H., Laskar, J., Monechi, S., Powell, J., Plumb, K.A., Raffi, I., Röhl, U., Sanfilippo, A., Schmitz, B., Shackleton, N.J., Shields, G.A., Strauss, H., Van Dam, J., Veizer, J., van Kolfschoten, Th., Wilson, D., 2004. A Geologic Time Scale 2004. Cambridge University Press. 500pp.

Gresse, P.G., Theron, J.N., Fitch, F.J., Miller, J.A., 1992. Tectonic inversion and radiometric resetting of the basement in the Cape Fold Belt. In: de Wit, M.J., Ransome, I.G.D. (Eds.), Inversion Tectonics of the Cape Fold Belt, Karoo and Cretaceous Basins of Southern Africa. Balkema, Rotterdam, pp. 217–228.

Gupta, S., Cowie, P.A., Dawers, N.H., Underhill, J.R., 1998. A mechanism to explain rift-basin subsidence and stratigraphic patterns through fault array-evolution. Geology 26, 595–598.

Hälbich, I.W., 1993. The Cape Fold Belt–Agulhas Bank transect across Gondwana Suture, Southern Africa. Global Geoscience Transect 9, American Geophysical Union, Publication No 202 of International Lithosphere Program, Washington, 18pp.

Hälbich, I.W., Fitch, F.J., Miller, J.A., 1983. Dating the Cape orogeny. In: Söhnge, A.P.G., Hälbich, I.W. (Eds.), Geodynamics of the Cape Fold Belt. Special Publication of the Geological Society of South Africa 12, pp. 149–164.

Harvey, J.D., de Wit, M.J., Stankiewicz, J., Doucouré, C.M., 2001. Structural variations of the crust in the Southwestern Cape, deduced from seismic receiver functions. South African Journal of Geology 104, 231–242.

Hubbard, R.J., Pape, J., Roberts, D.G., 1985a. Depositional sequence mapping as a technique to establish tectonic and stratigraphic framework and evaluate hydrocarbon potential on a passive continental margin. In: Beerg, O.R., Wooverton, D.G (Eds.), Seismic Stratigraphy II. American Association of Petroleum Geologists Memoir 29, pp. 79–92.

Hubbard, R.J., Pape, J., Roberts, D.G., 1985b. Depositional sequence mapping to illustrate the evolution of a passive continental margin. In: Beerg, O.R., Wooverton, D.G. (Eds.), Seismic Stratigraphy II. American Association of Petroleum Geologists Memoir 29, pp. 93–116.

Illies, J.H., 1981. Mechanism of graben formation. Tectonophysics 73, 249–266.

Jackson, J.A., White, N.J., 1989. Normal faulting in the upper continental crust: observations from regions of active extension. Journal of Structural Geology 11, 15–36.

Jackson, J.A., Blenkinsop, T., 1997. The Bilila–Mtakataka fault in Malawi: an active, 100-km-long, normal fault segment in thick seismogenic crust. Tectonics 16, 137–150.

Le Roux, J.P., 1983. Structural evolution of the Kango Group. In: Söhnge, A.P.G., Hälbich, I.W. (Eds.), Geodynamics of the Cape Fold Belt. Geological Society of South Africa Special Publication 12, pp. 47–56.

Lezzar, K.E., Tiercelin, J.J., LeTurdu, C., Cohen, A.S., Reynolds, D.J., LeGall, B., Scholz, C.A., 2002. Control of normal fault interaction on the distribution of major Neogene sedimentary depocenters, Lake Tanganyika, East African rift. Bulletin of the American Association of Petroleum Geologists 86, 1027–1059.

Machette, M.N., Personius, S.F., Nelson, A.R., Schwartz, D.P., Lund, W.R., 1991. The Wasatch fault zone, Utah—segmentation and history of Holocene earthquakes. Journal of Structural Geology 13, 137–149.

Marchal, D., Guiraud, M., Rives, T., Van den Driessche, J., 1998. Space and time propagation processes of normal faults. In: Jones, G., Fisher, Q.J., Knipe, R.J. (Eds.), Faulting, Fault Sealing and Fluid Flow in Hydrocarbon Reservoirs. Geological Society of London Special Publication 147, pp. 51–70.

McClay, K.R., Dooley, T., Whitehouse, P., Mills, M., 2002. 4-D evolution of rift systems: insights from scale physical models. Bulletin of the American Association of Petroleum Geologists 86, 935–959.

McConnell, R.B., 1972. Geological development of the rift system of Eastern Africa. Bulletin of the American Association of Petroleum Geologists 83, 2549–2572.

McLachlan, I.R., McMillan, I.K., 1976. Review and stratigraphic significance of Southern Cape Mesozoic Paleontology. Transactions of the Geological Society of South Africa 79, 197–212.

McLeod, A.E., Dawers, N.H., Underhill, J.R., 2000. The propagation and linkage of normal faults: insights from the Strathspey–Brent–Statfjord fault array, northern North Sea. Basin Research 12, 263–284.

McLeod, A.E., Underhill, J.R., Davies, S.J., Dawers, N.H., 2002. The influence of fault array evolution on syn-rift sedimentation patterns: controls on deposition in the Strathspey–Brent–Statfjord half-graben, Northern North Sea. Bulletin of the American Association of Petroleum Geologists 86, 1061–1094.

McMillan, I.K., Brink, G.J., Broad, D.S., Maier, J.J., 1997. Late Mesozoic sedimentary basins off the South Coast of South Africa. In: Selly, R.C. (Ed.), African Basins: Sedimentary Basins of the World 3. Elsevier, Amsterdam, pp. 319–376.

Mitchum Jr., R.M., Vail, P.R., Sangree, J.B., 1977. Seismic stratigraphy and global changes of sea-level part 6: seismic stratigraphic interpretation procedure. In: Payton, C.E. (Ed.), Seismic Stratigraphy—Applications to Hydrocarbon Exploration. Bulletin of the American Association of Petroleum Geologists Memoir 26, pp. 117–134.

Morley, C.K., 1999. Patterns of displacement along large normal faults: implications for basin evolution and fault propagation, based on examples from East Africa. Bulletin of the American Association of Petroleum Geologists 83, 613–634.

Newton, A.R., 1993. The Cape folding—a syntaxis or not? South African Journal of Geology 96, 213–216.

Paton, D.A., 2002. The evolution of southern South Africa: insights into structural inheritance and heterogeneous normal fault growth. PhD Thesis, University of Edinburgh.

Paton, D.A., Underhill, J.R., 2004. Role of crustal anisotropy in modifying the structural and sedimentological evolution of extensional basins: the Gamtoos Basin, South Africa. Basin Research 16, 339–359.

Prosser, S., 1993. Rift-related linked depositional systems and their seismic expression. In: Williams, G.D., Dobb, A. (Eds.), Tectonics and Seismic Sequence Stratigraphy. Geological Society London Special Publication 71, pp. 35–66.

Ramberg, I.B., 1978. The tectonic history of the Oslo Region. In: Ramberg, I.B. (Ed.), Tectonics and Geophysics of Continental Rifts. Reidel Publishing Company, Dordrecht, Holland, pp. 39–40.

Schlische, R.W., 1992. Structural and stratigraphic development of the Newark extensional basin, eastern North America; evidence for the growth of the basin and its bounding structures. Geological Society of American Bulletin 104, 1246–1263.

Schlische, R.W., Anders, M.H., 1996. Stratigraphic effects and tectonic implications of the growth of normal faults and extensional basins. In: Beratan, K.K. (Ed.), Reconstructing the History of Basin and Range Extension using Sedimentology and Stratigraphy. Geological Society of America Special Publication 303, pp. 183–203.

Schlische, R.W., Young, S.S., Ackermann, R.V., Gupta, A., 1996. Geometry and scaling of a population of very small scale rift-related normal faults. Geology 24, 683–686.

Sharp, I.R., Gawthorpe, R.L., Armstrong, B., Underhill, J.R., 2000. Propagation history and passive rotation of mesoscale normal faults: implications for syn-rift stratigraphic development. Basin Research 12, 285–305.

Shone, R.W., Nolte, C.C., Booth, P.W.K., 1990. Pre-Cape rocks of the Gamtoos area—a complex tectonostratigraphic package preserved as a horst block. South African Journal of Geology 93, 616–621.

Tankard, A.J., Jackson, M.P.A., Eriksson, K.A., Hobday, D.K., Hunter, D.R., Minter, W.E.L., 1982. Crustal Evolution of Southern Africa. Springer-Verlag, New York. 520pp.

Trudgill, B., Cartwright, J., 1994. Relay-ramp forms and normal-fault linkages, Canyonlands National Park, Utah. Geological Society of America Bulletin 106, 1143–1157.

Turner, B.R., 1999. Tectonostratigraphical development of the Upper Karooforeland basin: Orogenic unloading versus thermally-induced Gondwana rifting. Journal of African Earth Sciences 28, 215–238.

Veevers, J.J., Cole, D.I., Cowan, E.J., 1994. Southern Africa: Karoo Basin and Cape Fold Belt. In: Veevers, J.J., Powell, C.McA. (Eds.), Permian–Triassic Pangean Basins and Foldbelts Along the Panthalassan Margin of Gondwanaland. Geological Society of America Memoir, pp. 223–279.

Walsh, J.J., Nicol, A., Childs, C., 2002. An alternative model for the growth of faults. Journal of Structural Geology 24, 1669–1675.

Walsh, J.J., Watterson, J., 1988. Analysis of the relationship between displacements and dimensions of faults. Journal of Structural Geology 10, 239–247.